

Optimizing Anharmonicity in Nanoscale Weak Link Josephson Junction Oscillators

R. Vijay¹, J. D. Sau², Marvin L. Cohen², and I. Siddiqi¹

¹*Quantum Nanoelectronics Laboratory, Department of Physics,
University of California, Berkeley, CA 94720 and*

²*Department of Physics, University of California,
Berkeley, CA 94720 and Materials Sciences Division,*

Lawrence Berkeley National Laboratory, Berkeley, CA 94720

(Received textdate; Revised textdate; Accepted textdate; Published textdate)

Josephson tunnel junctions are widely used as nonlinear elements in superconducting circuits such as low noise amplifiers and quantum bits. However, microscopic defects in the oxide tunnel barrier can produce low and high frequency noise which can potentially limit the coherence times and quality factors of resonant circuits. Weak link Josephson junctions are an attractive alternative provided that sufficient nonlinearity can be engineered. We compute the current phase relation for superconducting weak links, with dimensions comparable to the zero temperature coherence length, connected to two and three dimensional superconducting electrodes. Our results indicate that 50-100 nm long aluminum nanobridges connected with three dimensional banks can be used to construct nonlinear oscillators for bifurcation amplification. We also show that under static current bias, these oscillators have a sufficiently anharmonic energy level structure to form a qubit. Such weak link junctions thus present a practical new route for realizing sensitive quantum circuits.

Nonlinear oscillators with low loss are a basic building block of superconducting quantum information processing circuits. They are used both as “artificial atoms” to realize quantum bits [1], and as the gain element in low noise amplifiers [2] for quantum state measurement. The Josephson tunnel junction, formed by separating two superconducting electrodes with a barrier such as a thin oxide layer [3], is the nonlinear circuit element commonly used to construct these anharmonic oscillators. The current $I(t)$ and voltage $V(t)$ of the junction can be expressed in terms of $\delta(t)$, the gauge-invariant phase difference, as $I(t) = I_0 \sin \delta(t)$ and $V(t) = \varphi_0 d\delta/dt$, where the parameter I_0 is the junction critical current and $\varphi_0 = \hbar/2e$ is the reduced flux quantum. These equations parameterize a nonlinear inductance $L_J = \varphi_0 / \{I_0 \cos(\delta)\}$. This Josephson inductance is shunted in parallel by a capacitance C_S resulting from the geometric capacitance of the junction and possibly an additional external capacitor, thereby forming an electrical oscillator with an amplitude dependent plasma oscillation frequency $\omega_P = 1/\sqrt{L_J(I)C_S}$. In principle, Josephson oscillators should exhibit a very large quality factor (Q) since at temperatures T well below the critical temperature T_c , dissipative thermal quasiparticle production is exponentially suppressed. In practice, microscopic defects in the tunnel barrier [4] and in the shunt capacitor dielectric [5] can reduce Q.

An alternative structure to the oxide barrier tunnel junction is a weak link Josephson junction (see [6] for a review) where a small metallic constriction with dimensions of order the superconducting coherence length $\xi(T)$ bridges two large superconducting electrodes. This type of junction also behaves as a nondissipative inductance but the strength of the nonlinearity is a sensitive function of the weak link and electrode geometry. In contrast to a tunnel junction which invariably has a sinusoidal current phase relation (CPR) with $I \propto \sin(\delta)$, a weak link junc-

tion at $T \ll T_c$ can exhibit a wide range of CPRs ranging from $I \propto \delta$ —characteristic of a linear inductor—to a distorted sinusoid $I \propto \cos(\delta/2) \tanh^{-1}[\sin(\delta/2)]$ for an idealized, short constriction [7]. In this letter, we present calculated CPRs, obtained via a numerical solution of the Usadel equations [8], for thin, diffusive superconducting bridges contacted with two and three dimensional banks for varying bridge length and width. We also compute the dynamics of a weak link Josephson oscillator under ac excitation, and its bound state energies. Our results indicate that with a 50-100nm long, 45nm wide aluminum bridge with three dimensional banks, the oscillator is sufficiently nonlinear to observe a stable dynamical bifurcation with a fixed frequency microwave drive, and to obtain three quantized levels with $\sim 3\%$ anharmonicity under dc bias. These results are obtained without putting impractical constraints on the shunting capacitance, oscillator quality factor, or current bias stability, and thus suggest a new route for realizing superconducting qubits and amplifiers without tunnel junctions. Furthermore, this junction geometry is suitable for coupling Josephson devices to other solid state quantum systems such as nanomagnets and quantum dots.

We consider two canonical weak link geometries: a “Dayem” bridge where the banks are the same thickness as the weak link and a “variable thickness bridge” where the banks are significantly thicker than the weak link. Considerable literature exists on both of these structures. As $T \rightarrow T_c$, the temperature dependent coherence length $\xi(T)$ diverges and mean field methods, such as Ginzburg-Landau theory [9], can be used to compute the magnitude and phase of the superconducting order parameter along the bridge and in the banks [10]. For qubits and low noise amplifiers, we are interested in operating the Josephson junction at $T \ll T_c$ to minimize quasiparticle loss. In this regime, linear response methods based on Gorkov functions have been applied to short

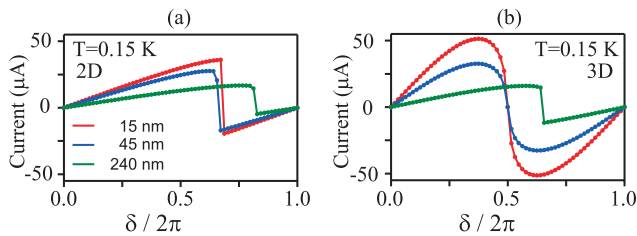


FIG. 1: Computed current phase relations for an Al nanobridge with width $W = 45$ nm and three different lengths $L = 15, 45,$ and 240 nm. Data are shown for (a) 2D and (b) 3D banks at $T = 0.15$ K. The 3D structures exhibit nonlinear CPRs which progressively become linear as L exceeds ξ . Corresponding lengths for 2D structures exhibit a nearly linear, hysteretic CPR (the other branch is suppressed for clarity). In both geometries, the maximum current systematically decreases with increasing bridge length.

weak links with length L and width $W \ll \xi(T)$, and with rigid boundary conditions imposed at the bridge ends — Kulik-Omelyanchuk (K-O) theory [7]. However, 10 – 30 nm thick Al bridges with a mean free path $l \sim 1$ nm [11] have $\xi(0) \approx 30$ nm, making the short limit difficult to achieve with conventional e-beam lithography. We thus focus on weak links with lateral dimensions comparable to $\xi(T = 0)$ and large compared to l . In the absence of closed form expressions for the CPR in this parameter regime, we apply the Nambu-Gorkov formalism [12, 13] in the diffusive limit and numerically solve the Usadel equations [8] for two and three dimensional weak link junctions.

We first compute the complex pairing potential Δ in the bridge and the banks. The modulus and argument of Δ yield the superconducting gap and phase, respectively. We use the Φ parametrization of the Usadel equations [14] by making the substitutions $F = \frac{\Phi}{\sqrt{\omega_n^2 + |\Phi|^2}}$ and $G^2 = 1 - |F|^2$ where G and F are the normal and anomalous Green's functions. This leads to the equations

$$g(\omega_n)(\Phi(\omega_n) - \Delta) = \frac{D_0}{2} \nabla [g(\omega_n)^2 \nabla \Phi(\omega)] \quad (1a)$$

$$g(\omega_n) = \frac{1}{\sqrt{\omega_n^2 + |\Phi(\omega, \mathbf{r})|^2}}, \Delta = \frac{\sum_n g(\omega_n) \Phi(\omega_n)}{\sum_n \frac{1}{\sqrt{\omega_n^2 + 1}}} \quad (1b)$$

where Δ and D_0 are the gap function and diffusion constant respectively, rescaled by Δ_0 , the zero temperature value of the gap. Finite temperature effects enter into the above equations through the spacing $\Delta\omega = 2\pi T/\Delta_0$ of the rescaled Matsubara frequencies ω_n . The Usadel equations are smooth in the frequency ω_n and hence the low temperature limit is expected to be reached when the temperature is about 10 times smaller than the gap $\Delta_0 = 1.764k_B T_C \approx 2.0$ K in Al. We find by comparing our numerical results in the K-O limit that an upper cutoff frequency of 8.0 K is sufficient for convergence. The equations are numerically solved self-consistently for Δ

and g on a 2D grid. For 3D structures, we use a cylindrically symmetric geometry to reduce it to an effective 2D problem. The solutions on the 2D grid are calculated for different values of superconducting phase difference across the device and the current density is calculated using

$$J(r) = \frac{\sigma}{e} \pi T \sum_{\omega} g(\omega)^2 \text{Im}(\Phi^*(\omega) \partial_x \Phi(\omega)) \quad (2)$$

where σ is the conductivity of the metal film, e is the electron charge and the gradients are computed along the length of the bridge.

The computed CPRs for an Al bridge with width $W = 45$ nm and three different lengths are shown in Fig. 1. Panels (a) and (b) compare bridges with 2D and 3D banks, respectively, at $T = 0.15$ K. We take $T_C = 1.2$ K. The banks for each bridge are 600 nm in each lateral dimension. For the 3D case, the banks also extend in the vertical direction as a hemi-cylinder of 600 nm diameter. For 3D structures, the CPR resembles a distorted sinusoid for the shortest bridge length $L = 15$ nm $\sim 0.5\xi(0)$. As the bridge length exceeds ξ , the current varies more linearly with the phase and the value of the maximum current decreases. A similar trend is seen for 2D structures of the same lateral dimension, but they exhibit a nearly linear CPR, even for $L < \xi(0)$. To validate our numerical simulation, we compared our result for a 15×15

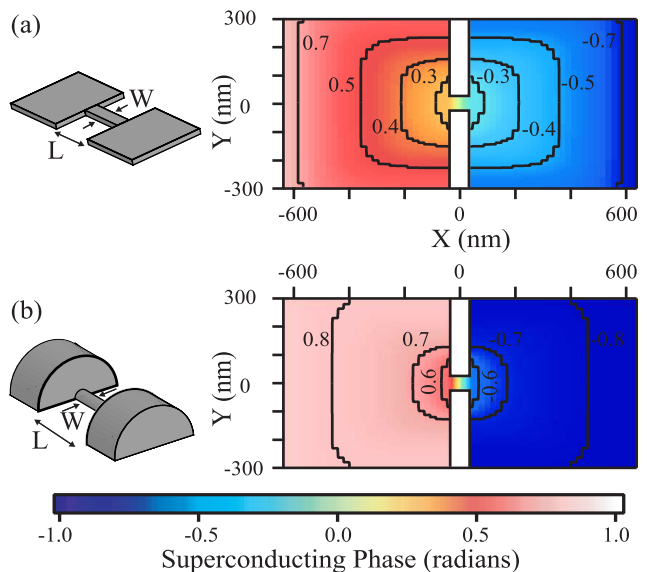


FIG. 2: Superconducting phase (color) as a function of position for an Al nanobridge with $L = 75$ nm and $W = 45$ nm. In (a) the banks are 2D with 600 nm lateral dimensions, and in (b) they are 3D as realized by a hemi-cylinder with 600 nm diameter. Contours of constant phase are also indicated. A total phase difference of 2 radians is imposed symmetrically across the bridge. In the 3D structure, most of the phase drop is across the constriction whereas in the 2D planar geometry, there is significant phase variation in the banks.

nm bridge contacted to ideal phase reservoirs with the analytical K-O result and found quantitative agreement. When computing the current for 2D devices, the bridge cross-sectional area was chosen to match that of the corresponding 3D devices by choosing the appropriate thickness for the 2D device. Note that the CPRs in general should be an odd function of δ and also be 2π periodic which leads to the requirement that the current should be zero at $\delta = \pm n\pi$ [14]. All the curves for the 2D device and that for $L = 240$ nm for the 3D device have a non-zero value of the current at $\delta = \pi$. However the full CPRs in these cases are multivalued and the other branch (suppressed in Fig. 1 for clarity) goes through zero at $\delta = \pi$.

In order to understand the different shape of the CPR in the 2D and 3D geometries, we plot in Fig. 2 the superconducting phase as a function of position in a 75 nm long, 45 nm wide weak link junction—dimensions readily achieved with e-beam lithography. For these plots, a phase difference of 2 radians is imposed symmetrically at the ends of the banks ($X = \pm 637.5$ nm) and variation with position is calculated. The phase is indicated by color and contour lines in Fig. 2. In the 3D case, the phase varies mostly in the bridge region and quickly heals to the imposed value in the banks within a few $\xi(0)$. Thus, the banks act as good phase reservoirs and the structure has a nonlinear CPR. In contrast, for the 2D case, the phase evolves both in the bridge and the banks, with a logarithmic approach to the imposed value at the boundaries. Since the banks fail to act as phase reservoirs, the entire structure resembles a superconducting wire with a linear CPR rather than a Josephson junction. This is particularly a problem when multiple 2D bridges are incorporated in a more complicated circuit like a SQUID loop. There is significant overlap of the weak link phases resulting in reduced modulation depth [10]. Some of these limitations of 2D Dayem bridges have been discussed in [6]. Variable thickness bridges are thus a more appropriate replacement for tunnel junctions.

We now consider both classical and quantum anharmonic oscillators formed by capacitively shunting a 3D weak link junction. We neglect the small intrinsic capacitance of the nanobridges [6] and assume that the plasma frequency is determined by the additional shunting capacitance only. For the classical case, we compute the oscillating junction voltage under a microwave drive. We consider a simple oscillator model where a weak link with generalized CPR $I(\delta) = I_0 f(\delta)$ with $\max |f(\delta)| = 1$ is shunted in parallel with a capacitance C_S and a real impedance R_S which sets the quality factor of the oscillator. The oscillator is driven with a time dependent current $I(t) = I_{RF} \cos(\omega_d t)$. The resulting equation of motion is

$$C_S \varphi_0 \frac{d^2 \delta(t)}{dt^2} + \frac{\varphi_0}{R_S} \frac{d\delta(t)}{dt} + I_0 f(\delta(t)) = I_{RF} \cos(\omega_d t) \quad (3)$$

The equation of motion was solved numerically using a fourth order Runge-Kutta method for CPRs correspond-

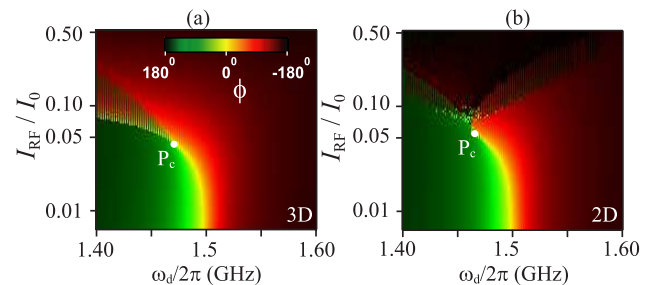


FIG. 3: Microwave frequency response of a nonlinear oscillator constructed using an Al nanobridge with $L = 75$ nm, $W = 45$ nm connected to (a) 3D and (b) 2D banks. The oscillator is driven with a single frequency ω_d . The phase ϕ of the steady state current oscillations, for a reflection setup, is plotted as a function of ω_d and normalized drive current I_{RF}/I_0 . Increasing and decreasing current sweeps are interlaced to highlight the hysteretic bistable region. Both devices exhibit pulling of the resonant frequency (yellow) to lower values with increasing drive current, typical of a driven nonlinear oscillator with a softening potential. However, beyond the critical point P_c (white dot), only the 3D device exhibits a well defined bistable region (striped) where the oscillations are confined to a single well of the periodic potential.

ing to nanobridges with $W = 45$ nm, $L = 75$ nm contacted with 2D and 3D banks. The CPRs for these two devices differ in the maximum current I_0 and the zero bias inductance $L_{J0} = \varphi_0 (\partial I(\delta)/\partial \delta)^{-1}|_{\delta=0}$. We chose values of C_S and R_S to obtain a small oscillation resonant frequency of 1.5 GHz and a quality factor $Q = 50$ for both samples—typical parameters in bifurcation amplifier circuits [15]. The results of the simulation are shown in Fig. 3a,b. The steady state oscillation phase, measured in reflection, is plotted in color as a function of drive frequency ω_d and normalized drive current I_{RF}/I_0 . Let us consider the variable thickness bridge first. At low drive amplitude $I_{RF}/I_0 < 0.01$, one recovers the familiar linear resonance behavior as the phase evolves from 180 to -180 degrees. The zero crossing of the phase (yellow) corresponds to the resonant frequency. As one drives the oscillator with larger drive current, the resonance frequency shifts to lower values as is expected for a softening potential. For currents beyond a critical value P_c , indicated as a white dot in the figure, the oscillator becomes bistable and can coexist in two dynamical states (dashed region). This behavior is typical of driven nonlinear oscillators [16] and has been experimentally verified in Josephson tunnel junction based oscillators [17]. This suggests that nanobridges with 3D banks can be used for potential applications in the field of bifurcation and parametric amplification [18]. On the other hand, we do not observe a well defined bistable region in the microwave response of the Dayem bridge structure. This is because accessing the nonlinear regime requires larger phase excursions and the phase δ can hop between neighboring wells of the periodic potential [19]. The critical point

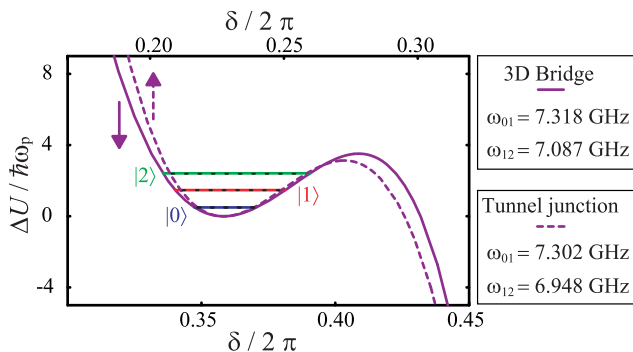


FIG. 4: Quantum energy levels in a current biased, capacitively shunted $L = 75$ nm, $W = 45$ nm Al nanobridge with 3D banks. For comparison, the potential and energy levels of a tunnel junction with the same critical current are shown as dashed lines. A current bias equal to 99% of the critical current is applied to obtain 3 quantum levels in the metastable potential well. The shunting capacitances are chosen to yield identical plasma frequencies. The level anharmonicity for the weak link junction ($\sim 3\%$) is only slightly smaller than that of the tunnel junction ($\sim 5\%$).

can be pushed to lower drive currents but this requires significantly higher values of Q .

Finally, we consider the possibility of constructing a quantum bit using weak link junctions. Since the critical current of these junctions tends to be large ($\sim 20\mu A$), it is natural to consider a phase qubit geometry in analogy with tunnel junction circuits with μA critical currents[20]. We will only present results for a 3D weak link junction and compare it with a Josephson tunnel junction since nanobridges with 2D banks have multivalued CPRs which complicates calculations and the potential operation of such a qubit. For the purpose of comparison, we also numerically solve the Schrödinger equation of capacitively shunted current biased Josephson junctions and find the quantum bound state energy levels. We choose a tunnel junction with a critical current equal to that of the weak link junction. An appropriate shunting capacitance is used to fix the zero bias plasma frequency of the tunnel junction device to $\omega_{P0}/2\pi = 20$ GHz. A static current bias equal to 99% of I_0 is used to tilt the washboard potential to reduce the plasma frequency to about 7.5 GHz, which is typical for phase qubits [20]. The 3D bridge with $L = 75$ nm and $W = 45$ nm is capacitively shunted to achieve the same reduced plasma

frequency under identical current bias.

The potential wells and bound state energies are shown in Fig. 4. The tunnel junction data are shown as dashed lines. The overall shape of the potential for the two cases is quite similar. The positions of the minima occur at different values of δ , as indicated by two horizontal axes in the figure, since the maximum in the CPR of the tunnel junction is at $\delta = \pi/2$ and at $\delta > \pi/2$ for the weak link junction. The lowest bound states have nearly the same energy with the subsequent higher levels differing by a few percent. For the tunnel junction, $\omega_{01} = 7.302$ GHz and $\omega_{12} = 6.948$ GHz, corresponding to an anharmonicity of $\sim 5\%$. For the weak link junction, $\omega_{01} = 7.318$ GHz and $\omega_{12} = 7.087$ GHz, corresponding to an anharmonicity of $\sim 3\%$, which is only slightly smaller than that of the tunnel junction and suggests the plausibility of weak link phase qubits. Moreover, it is possible to increase the anharmonicity by using a slightly higher plasma frequency.

In conclusion, we have investigated the microwave transport properties and quantum energy level structure of weak link Josephson junction oscillators, focusing in particular on optimizing anharmonicity. We computed the CPR for 2D Dayem and 3D variable thickness bridges by solving the Usadel equations for different bridge dimensions. The 3D structures exhibit strong nonlinearity—a consequence of the fact that the phase drop in these structures is confined mainly to the weak link. Under microwave drive, these junctions should exhibit bifurcation phenomenon for practical bridge dimensions and oscillator quality factor. Additionally, under static current bias, the quantum energy levels closely mimic ideal tunnel junction behavior, suggesting the possibility of constructing phase qubits without any lossy oxide barriers, giving potentially enhanced coherence. Nanobridge junctions proposed here can also potentially be used to couple superconducting circuits to other solid state quantum systems such as molecular magnets and quantum dots.

We would like to thank D.-H. Lee, B. Spivak, F. Wilhelm, R. Packard, M. Hatridge and J. Clarke for useful discussions. R.V. and I. S. acknowledge support from AFOSR Grant #: FA9550-08-1-0104. J. D. S and M. L. C. acknowledge support from NSF Grant No. DMR07-05941 and Director, Office of Science, Office of Basic Energy Sciences, Materials Sciences and Engineering Division, of the U.S. Department of Energy under contract No. DE-AC02-05CH11231.

-
- [1] M. H. Devoret, A. Wallraff, and J. M. Martinis, arXiv:cond-mat/0411174v1 (2007).
 [2] A. A. Clerk, M. H. Devoret, S. M. Girvin, F. Marquardt, and R. J. Schoelkopf, arXiv:0810.4729v1 (2008).
 [3] B. D. Josephson, Rev. Mod. Phys. **36**, 216 (1964).
 [4] R. W. Simmonds, K. M. Lang, D. A. Hite, S. Nam, D. P.

- Pappas, and J. M. Martinis, Phys. Rev. Lett. **93**, 077003 (2004).
 [5] J. M. Martinis, K. B. Cooper, R. McDermott, M. Steffen, M. Ansmann, K. D. Osborn, K. Cicak, S. Oh, D. P. Pappas, R. W. Simmonds, et al., Phys. Rev. Lett. **95**, 210503 (2005).

- [6] K. K. Likharev, *Rev. Mod. Phys.* **51** (1979).
- [7] I. O. Kulik and A. N. Omel'Yanchuk, *Soviet JETP* **21**, 96 (1975).
- [8] K. D. Usadel, *Phys. Rev. Lett.* **25** (1970).
- [9] V. L. Ginzburg and L. D. Landau, *Zh. Eksp. Teor. Fiz.* **20**, 1064 (1950).
- [10] K. Hasselbach, D. Mailly, and J. R. Kirtley, *J. Appl. Phys.* **91**, 4432 (2002).
- [11] I. Siddiqi, A. Verevkin, D. E. Prober, A. Skalare, W. R. McGrath, P. M. Echternach, and H. G. LeDuc, *J. Appl. Phys.* **91**, 4646 (2002).
- [12] L. P. Gor'kov, *Zh. Eksp. Teor. Fiz.* **34**, 735 (1958).
- [13] Y. Nambu, *Phys. Rev.* **117** (1960).
- [14] A. A. Golubov, M. Y. Kupriyanov, and E. Il'ichev, *Rev. Mod. Phys.* **76** (2004).
- [15] I. Siddiqi, R. Vijay, F. Pierre, C. M. Wilson, M. Metcalfe, C. Rigetti, L. Frunzio, and M. H. Devoret, *Phys. Rev. Lett.* **93**, 207002 (2004).
- [16] L. D. Landau and E. M. Lifshitz, *Small Oscillations* (Pergamon Press, 1960), chap. V, Mechanics.
- [17] I. Siddiqi, R. Vijay, F. Pierre, C. M. Wilson, L. Frunzio, M. Metcalfe, C. Rigetti, R. J. Schoelkopf, M. H. Devoret, D. Vion, et al., *Phys. Rev. Lett.* **94**, 027005 (2005).
- [18] B. Yurke, L. R. Corruccini, P. G. Kaminsky, L. W. Rupp, A. D. Smith, A. H. Silver, R. W. Simon, and E. A. Whittaker, *Phys. Rev. A* **39**, 2519 (1989).
- [19] V. E. Manucharyan, E. Boaknin, M. Metcalfe, R. Vijay, I. Siddiqi, and M. Devoret, *Phys. Rev. B* **76**, 014524 (2007).
- [20] J. M. Martinis, S. Nam, J. Aumentado, and C. Urbina, *Phys. Rev. Lett.* **89**, 117901 (2002).